IEEE Access
Multidisciplinary | Rapid Review | Open Access Journal

Received 8 August 2024, accepted 23 August 2024, date of publication 27 August 2024, date of current version 4 September 2024.

Digital Object Identifier 10.1109/ACCESS.2024.3450602

APPLIED RESEARCH

Dynamic Calibration Based on the Black-Scholes Option Pricing Model by Bayesian Method

NORRIS M. MULENGA AND YU FU
College of Mathematics and Systems Science, Shandong University of Science and Technology, Qingdao 266590, China
Corresponding author: Yu Fu (fuyu@sdust.edu.cn)

This work was supported in part by the National Natural Science Foundations of China under Grant 11701335, and in part by the Natural Science Foundation of Shandong Province under Grant ZR2017BA016.

ABSTRACT To improve the shortcomings of the classic Black-Scholes model, mainly on the constant volatility and normal distribution assumptions, this paper investigates the dynamic calibration method, which makes the expected return rate, volatility and interest rate become data-driven and time dependent. Based on the dynamic procedure, four distinct calibration models are proposed by using Bayesian method, among which Model I and Model II are used for comparison, Model III simultaneously uses the data of underlying asset, put and call options by introducing the bivariate normal distribution, and Model IV simplifies Model III by employing the put-call parity. The results of numerical experiments and empirical analysis illustrate that Model III is the most accurate but time consuming, while Model IV is the most efficient. Dynamic calibration method is also verified to be much more accurate in data fitting and option pricing than the commonly used global calibration. Overall, the dynamically calibrated Black-Scholes model can be regarded as an improvement on the classic Black-Scholes model, where model coefficients are functions of time. As a result, leptokurtic and negative skew distribution of log returns is regenerated, which makes the model more consistent with the data observed in real markets without an increase of the complexity.

INDEX TERMS Bayesian method, dynamic calibration, Black-Scholes model, Markov Chain Monte Carlo, volatility surface, leptokurtosis.

I. INTRODUCTION

The Black-Scholes model [1], developed by Fischer Black and Myron Scholes in the early 1970s, revolutionized the field of quantitative finance by providing a mathematical framework for pricing European options. However, despite its widespread adoption and enduring influence, the Black-Scholes model is not without its limitations, among which the normal distribution and constant volatility assumptions are of the most concern [2]. As a result, two empirical phenomena from financial markets, the asymmetric leptokurtic distribution of returns and the volatility smile/skew, can not be replicated from the Black-Scholes model. To develop more consistent models, modifications of the Black-Scholes model have been extensively studied, including but not limited to stochastic and local volatility models [3], [4], [5], [6], jump-diffusion models [2], [7], [8], GARCH models [9], [10], rough volatility models [11], [12], neural-SDE models [13] and signature-based models [14], [15].

Model calibration is a necessary and important step before the application of option pricing models to the real market. However, as accurate but complicated models keep emerging, the problem of calibrating the model parameters is getting increasingly difficult. Traditionally, there are two main methods for model calibration, parametric method and non-parametric method. In the parametric method, authors usually obtain estimations of model parameters based on the historical data from financial markets, such as maximum likelihood estimation [16], and Bayesian estimation [17], [18], [19]. For the non-parametric method, parameters are often approximated by some regularized optimization methods to deal with the ill-posed inverse problem, for example, Tikhonov-type regularization method [20], [21], [22]

The associate editor coordinating the review of this manuscript and approving it for publication was Vlad Diaconita.

and relative entropy method [23], [24], [25]. Besides, some researchers also resort to partial differential equation based method [26], [27] to obtain the approximate values by iterations. Most recently, machine learning and neural networks are also devoted to both modeling and calibration with their fast development [28], [29], [30].

In this work, a dynamic calibration method is proposed based on the classic Black-Scholes model, estimating the model parameters by Bayesian method. By continuously updating the dataset used for calibration, the calibrated model parameters become time dependent, which makes the dynamically calibrated model more consistent with the real market. To further enhance the accuracy of model calibration, different types of available data are exploited in this dynamic procedure. Inspired by local volatility models, put and call options with the same maturity and strike price share common model parameters, including expected return rate, volatility and interest rate. Thus, the prices of underlying assets, put and call options are combined together in our dynamic calibration to improve the accuracy of parameter estimation. In this paper, Bayesian method is adopted for its robustness and flexibility, as well as its natural way to derive the interval estimates for model parameters, which plays an important role in analyzing the accuracy of option price prediction.

To illustrate the superiority of the proposed method, four different parameter calibration models are constructed, among which Model I only uses data from underlying assets, Model II incorporates both underlying asset and call option data, while Model III and Model IV utilize data from underlying assets, put and call options. More specifically, Model IV is a modification of Model III by means of the put-call parity, which significantly improves the efficiency while maintaining a certain level of accuracy.

In fact, with the rapid development of the computational power and artificial intelligence, research on parameter calibration based on various types of data keeps emerging constantly [14], [15], [27], [31]. Specifically, in signature-based models, spot prices as well as the data from vanilla and exotic options can be combined together to implement a more precise joint calibration. In comparison with these studies, the contributions of this paper are summarized as follows.

1) EFFICIENCY OF CALIBRATION TO PUT AND CALL OPTIONS

The proposed dynamic calibration method is efficient because on the one hand the standard Black-Scholes model is quite simple. On the other hand, the size of the calibration dataset is relatively small. These two features dramatically accelerate the process of finding the maximum a posteriori estimation (MAPE) and the sampling by Markov Chain Monte Carlo (MCMC). Moreover, the efficiency is further improved by exploiting the put-call parity in Model IV.

2) MARKET CONSISTENCY

In our empirical analysis, the asymmetric leptokurtic distribution of returns and the volatility skew are observed from the calibrated model, which is consistent with real financial markets and a significant improvement of the standard Black-Scholes model.

3) ACCURATE IN OPTION PRICING AND PRICE PREDICTION FOR OUT-OF-SAMPLE DATA

Unlike the literature mentioned above, the empirical analysis in this work not only validates the accuracy of data fitting, but also examines the precision of option pricing and price prediction for out-of-sample data, indicating that the proposed dynamic calibration method exhibits good generalization ability.

4) COMPUTATION OF INTERVAL ESTIMATION

One of the most important advantages of Bayesian method is that the interval estimates can be computed according to the samples from the posterior distribution. In this paper, highest posterior density intervals (HPDI) are calculated as predictions for the future option prices, not just a predicted value.

The remainder of this paper is structured as follows: In Section II we introduce four different calibration models and the dynamic procedure. Then numerical experiments are carried out in Section III based on simulated data. Section IV is dedicated to our empirical analysis of the daily data of SPX options from 16th September, 2022 to 8th September, 2023 with different strike prices and the same maturity on 15th September, 2023. Finally, Section V concludes our work by summarizing key findings and offering valuable recommendations for future research directions.

To explain the meaning of abbreviations used in the paper clearly, a list of commonly used nomenclatures are provided in the following table for easy reference by readers.

TABLE 1. Nomenclatures.

Nomenclatures	Referred to
EAPE	Expected A Posteriori Estimation
ESS	Effective Sample Size
HPDI	Highest Posterior Density Interval
LKJ	Lewandowski-Kurowicka-Joe
LSTM	Long Short-Term Memory
MAPE	Maximum A Posteriori Estimation
MCMC	Markov Chain Monte Carlo
MCSE	Monte Carlo Standard Error
NUTS	No-U-Turn Sampler
PDF	Probability Density Function
PSTD	Posterior Standard Deviation
RMSE	Root Mean Square Error
RMSRE	Root Mean Square Relative Error
SD	Standard Deviation
SDE	Stochastic Differential Equation
SPX	Standard & Poor's 500 Index

II. MODEL CONSTRUCTION AND DYNAMIC CALIBRATION

The dynamic calibration method proposed in this paper is based on the standard Black-Scholes model. Let $(\Omega, \{\mathcal{F}_t\}_{t\in[0,T]}, \mathcal{F}, \mathbb{P})$ denote a probability space, where

$\{\mathcal{F}_t\}_{t\in[0,T]}$ is the natural filtration of standard Brownian motion B_t. The dynamics of the asset price S_t follows the stochastic differential equation (SDE)

$$\begin{cases} \mathrm{d}S_t = \mu S_t \mathrm{d}t + \sigma S_t \mathrm{d}B_t, \quad t \in (0, T] \\ S_t|_{t=0} = S_0, \end{cases} \tag{1}$$

where μ and σ are assumed to be constants, denoting the expected return rate and the volatility, respectively. By the principle of risk-neutral pricing, the Black-Scholes model yields an explicit pricing formula for European call and put options, that is,

$$\begin{aligned} \hat{C}_t &= \hat{C}(t, S_t) = N(d_1)S_t - N(d_2)Ke^{-r\tau}, \\ \hat{P}_t &= \hat{P}(t, S_t) = N(-d_2)Ke^{-r\tau} - N(-d_1)S_t, \end{aligned} \tag{2}$$

where $N(x)$ denotes the cumulative distribution function of the standard normal distribution, $\tau = T - t$ is the remaining time to the maturity, K signifies the strike price, r is a constant representing the risk-free interest rate, d_1 and d_2 are defined as

$$\begin{aligned} d_1 &= \frac{1}{\sigma\sqrt{\tau}}\left(\log\left(\frac{S_t}{K}\right) + \left(r + \frac{\sigma^2}{2}\right)\tau\right), \\ d_2 &= d_1 - \sigma\sqrt{\tau}. \end{aligned}$$

From the Black-Scholes formula for call and put options (2), the factors influencing the price of European options include the current price of the underlying asset, strike price, time to maturity, risk-free interest rate and volatility, while the expected return rate does not appear in the pricing formula.

The put-call parity is based on the principle of arbitrage-free pricing, that is, two portfolios that always have the same payoff at time T must have the same value at any prior time. Under this assumption, the price of European call and put options with the same underlying asset, strike price and maturity must satisfy the following condition:

$$C(t, S_t) - P(t, S_t) = S_t - Ke^{-r\tau}. \tag{3}$$

It is worth to note that the Black-Scholes formula (2) also holds in a arbitrage-free market, which means that call and put option prices derived by Black-Scholes formula satisfy the put-call parity.

Under the framework of the Black-Scholes model, we propose four distinct calibration models and introduce our dynamic calibration method in this section. In each model, parameters are estimated by Bayesian method, obtaining their posterior density by the Bayes' theorem

$$p(\theta|\mathcal{D}) = \frac{p(\theta)\cdot p(\mathcal{D}|\theta)}{p(\mathcal{D})}, \tag{4}$$

where θ represents parameters to be estimated, $\mathcal{D}$ is a given dataset, $p(\theta), p(\mathcal{D}), p(\mathcal{D}|\theta)$ and $p(\theta|\mathcal{D})$ are known as the prior distribution, evidence, likelihood function and posterior distribution, respectively. However, the evidence, which can be expressed as

$$p(\mathcal{D}) = \int_\Theta p(\theta)\cdot p(\mathcal{D}|\theta)\mathrm{d}\theta,$$

is a multi-dimensional integral that even complicated to approximate in most practical situations, where Θ denotes the parameter space. Thus we resort to the well-known Markov Chain Monte Carlo method [32], [33], [34] to draw samples from the posterior distribution while circumventing the evaluation of $p(\mathcal{D})$. Specifically, the No-U-Turn Sampler (NUTS) [35] is employed in the proposed four models.

Before introducing our calibration models, we define the following notations on the dataset. Suppose that data on the prices of underlying assets, call options and put options in the financial market can be periodically observed at times $t_i \in [0, T]$, with the time interval size Δt. Let D_t^S, D_t^C and D_t^P denote the datasets of spot prices, call option prices and put option prices before time t, respectively. That is,

$$\mathcal{D}_t^S = \{(t_i, S_{t_i})\}_{t_i\le t}, \mathcal{D}_t^C = \{(t_i, C_{t_i})\}_{t_i\le t}, \mathcal{D}_t^P = \{(t_i, P_{t_i})\}_{t_i\le t}.$$

A. MODEL I: SPOT PRICES MODEL

Model I is a naive model to estimate parameters $\theta_1 = (\mu, \sigma)$ on the dataset $\mathcal{D}_t^S$. From the Black-Scholes model (1) and the Itô formula, we can easily deduce the log returns of the underlying assets follow a normal distribution, which is,

$$R_{t_i} = \log\left(\frac{S_{t_i+1}}{S_{t_i}}\right) \sim \mathcal{N}\left((\mu - \frac{1}{2}\sigma^2)\Delta t, \sigma^2\Delta t\right). \tag{5}$$

Thus we can write the likelihood function as

$$L(\mathcal{D}_t^S|\theta_1) = \prod_{t_i\le t}\phi\left(\log\left(\frac{S_{t_i+1}}{S_{t_i}}\right) - \left(\mu - \frac{1}{2}\sigma^2\right)\Delta t \,\middle|\, \sigma^2\Delta t\right),$$

where $\phi(\cdot|\sigma^2)$ denote the probability density function (PDF) of $N(0, \sigma^2)$. Then by setting the priors as

$$\mu \sim N(0, \delta_\mu^2), \quad \sigma \sim N^+(\delta_\sigma),$$

the posterior distribution of θ_1 can be derived as

$$p(\theta_1|\mathcal{D}_t^S) \propto \phi(\mu|\delta_\mu^2)\cdot\phi^+(\sigma|\delta_\sigma)\cdot L(\mathcal{D}_t^S|\theta_1), \tag{6}$$

where $N^+(\delta)$ denotes half-normal distribution with parameter δ, $\phi^+(\cdot|\delta)$ denotes the PDF of $N^+(\delta)$.

Remark 1: In Bayesian analysis, the posterior distribution has a strong reliance on the prior distribution. How to select reasonable prior distributions for different models is a major concern in many researches, which is beyond the discussion of this work. Interested readers may refer to [32] and [36] for more information. In this paper, we assume that the prior distributions of parameters are mutually independent and set them to be normal or half normal distributions with large variance, which can be regarded as weakly informative priors [32].

B. MODEL II: COMBINED WITH CALL OPTION PRICES

One of the major drawbacks of Model I in option pricing is that it does not estimate the (implied) risk-free interest, which is a key parameter in pricing formula (2). To this point, Model

II is built based on the dataset $\mathcal{D}_t^S \cup D_t^C$. Similar to the analysis in [31], the call option price in the real market C_{t_i} can be expressed as

$$C_{t_i} = \hat{C}_{t_i} + \varepsilon_{t_i}^c, \quad \varepsilon_{t_i}^c \sim N(0, \tau_i \sigma_c^2), \tag{7}$$

where $\tau_i = T - t_i$ and $\hat{C}_{t_i}$ denotes the Black-Scholes price in (2). There are many reasons for the presence of error terms $\varepsilon_{t_i}^c$, such as the market liquidity, supply-demand levels and bid-ask prices. As our assumption, the theoretical option price is determined by the Black-Scholes formula, leading to the zero mean of $\varepsilon_{t_i}^c$. Moreover, the impact affecting the error term diminishes in influence as the maturity date approaches, so we introduced a factor τ_i into the variance term.

Denote the parameters to be estimated in Model II by $\theta_2 = (\mu, \sigma, r, \sigma_c)$, the likelihood function in Model II can be obtained according to (7), that is,

$$\begin{aligned} &L(\mathcal{D}_t^S \cup \mathcal{D}_t^C | \theta_2) \\ &\quad = L(\mathcal{D}_t^S | \theta_2) \cdot L(\mathcal{D}_t^C | \theta_2, \mathcal{D}_t^S) \\ &\quad = L(\mathcal{D}_t^S | \theta_1) \cdot \prod_{t_i \le t} \phi(C_{t_i} - \hat{C}(t_i, S_{t_i}) | \tau_i \sigma_c^2). \end{aligned} \tag{8}$$

Setting the priors by

$$\mu \sim N(0, \delta_\mu^2), r \sim N(0, \delta_r^2), \sigma \sim N^+(\delta_\sigma), \sigma_c \sim N^+(\delta_c),$$

we derive the posterior distribution of θ_2 as

$$\begin{aligned} p(\theta_2 | \mathcal{D}_t^S \cup \mathcal{D}_t^C) \propto \phi(\mu | \delta_\mu^2) \cdot \phi^+(\sigma | \delta_\sigma) \cdot \phi(r | \delta_r^2) \\ \cdot \phi^+(\sigma_c | \delta_c) \cdot L(\mathcal{D}_t^S \cup \mathcal{D}_t^C | \theta_2) \end{aligned} \tag{9}$$

Remark 2: If the priors in Model II is set to be uniform distribution, then the posterior PDF can be simplified to

$$p(\theta_2 | \mathcal{D}_t^S \cup \mathcal{D}_t^C) \propto L(\mathcal{D}_t^S | \theta_2) \cdot L(\mathcal{D}_t^C | \theta_2, \mathcal{D}_t^S).$$

Regarding $L(\mathcal{D}_t^S | \theta_2)$ as a prior distribution of θ_2 from the past information of spot prices, then $p(\theta_2 | \mathcal{D}_t^S \cup \mathcal{D}_t^C)$ updated the prior with the information of call option prices.

C. MODEL III: COMBINED WITH CALL AND PUT OPTIONS

In this model, we try to combine the data from underlying assets, put and call options together to obtain the posterior PDF of model parameters on the dataset $\mathcal{D}_t^S \cup \mathcal{D}_t^C \cup \mathcal{D}_t^P$. Similar to the discussions in Model II, the corresponding put option prices, with the same strike price and maturity to the call option, can be expressed as

$$P_{t_i} = \hat{P}_{t_i} + \varepsilon_{t_i}^p, \quad \varepsilon_{t_i}^p \sim N(0, \tau_i \sigma_p^2),$$

where the definition of $\hat{P}_{t_i}$ comes from (2). In consideration of the correlation between $\varepsilon_{t_i}^c$ and $\varepsilon_{t_i}^p$, we propose that

$$\begin{bmatrix} C_{t_i} \\ P_{t_i} \end{bmatrix} = \begin{bmatrix} \hat{C}_{t_i} \\ \hat{P}_{t_i} \end{bmatrix} + \begin{bmatrix} \varepsilon_{t_i}^c \\ \varepsilon_{t_i}^p \end{bmatrix}, \tag{10}$$

where

$$\begin{bmatrix} \varepsilon_{t_i}^c \\ \varepsilon_{t_i}^p \end{bmatrix} \sim N(0, \tau_i \Sigma), \quad \Sigma = \begin{bmatrix} \sigma_c^2 & \rho \sigma_c \sigma_p \\ \rho \sigma_c \sigma_p & \sigma_p^2 \end{bmatrix}.$$

Thus the parameters to be estimated in Model III is denoted by $\theta_3 = (\mu, \sigma, r, \sigma_c, \sigma_p, \rho)$. And the likelihood function can be obtained as

$$\begin{aligned} &L(\mathcal{D}_t^S \cup \mathcal{D}_t^C \cup \mathcal{D}_t^P | \theta_3) \\ &\quad = L(\mathcal{D}_t^S | \theta_3) \cdot L(\mathcal{D}_t^C \cup D_t^P | \theta_3, \mathcal{D}_t^S) \\ &\quad = L(\mathcal{D}_t^S | \theta_1) \cdot \prod_{t_i \le t} \phi^*((C_{t_i} - \hat{C}_{t_i}, P_{t_i} - \hat{P}_{t_i}) | \tau_i \Sigma), \end{aligned}$$

where $\phi^*(\cdot, \cdot | \Sigma)$ denotes the PDF of two-dimensional normal distribution with mean zero and covariance matrix Σ. To choose a reasonable prior distribution for Σ, we decomposed the covariance matrix as

$$\Sigma = S \cdot C \cdot S, \quad \text{where } S = \text{diag}(\sigma_c, \sigma_p), C = \begin{bmatrix} 1 & \rho \\ \rho & 1 \end{bmatrix}.$$

Then we set

$$\sigma_c \sim N^+(\delta_c), \quad \sigma_p \sim N^+(\delta_p), \quad C \sim LKJ(\eta),$$

where $LKJ(\eta)$ denotes the Lewandowski-Kurowicka-Joe distribution [37] with parameter η. By selecting the priors of μ, σ, r as the same as Model II and an assumption of mutual independence, we get

$$\begin{aligned} &p(\theta_3 | \mathcal{D}_t^S \cup \mathcal{D}_t^C \cup \mathcal{D}_t^P) \\ &\quad \propto \phi(\mu | \delta_\mu^2) \cdot \phi^+(\sigma | \delta_\sigma) \cdot \phi(r | \delta_r^2) \cdot \phi^+(\sigma_c | \delta_c) \\ &\quad \cdot \phi^+(\sigma_p | \delta_p) \cdot \rho(C | \eta) \cdot L(\mathcal{D}_t^S \cup \mathcal{D}_t^C \cup \mathcal{D}_t^P | \theta_3), \end{aligned} \tag{11}$$

where

$$\rho(C | \eta) \propto [\det(C)]^{\eta - 1} \propto (1 - \rho^2)^{\eta - 1}$$

denotes the PDF of $LKJ(\eta)$.

D. MODEL IV: EXPLOITING THE PUT-CALL PARITY

In Model III, the posterior distribution of model parameters is derived under reasonable assumptions. However, the use of multivariant normal distribution makes the inference procedure much more complicated, especially for the covariance matrix Σ. Therefore, we are attempting to modify Model III by simplifying the model structure.

Unlike the straight forward way expressed in (10), the dataset $\mathcal{D}_t^P$ is incorporated in Model IV through the put-call parity conditional on $\mathcal{D}_t^C$, which is

$$\begin{aligned} &C_{t_i} = \hat{C}_{t_i} + \varepsilon_{t_i}^c, \quad \varepsilon_{t_i}^c \sim N(0, \tau_i \sigma_c^2), \\ &P_{t_i} = C_{t_i} - S_{t_i} + K e^{-r\tau_i} + \varepsilon_{t_i}^p, \quad \varepsilon_{t_i}^p \sim N(0, \tau_i \sigma_p^2), \end{aligned} \tag{12}$$

where $\varepsilon_{t_i}^p$ is the error in the put-call parity, S_{t_i}, C_{t_i} and P_{t_i} denotes the market prices of underlying asset, call and put option at t_i, respectively. Although the put-call parity holds exactly in arbitrage-free markets, data from real markets always contains arbitrage [38], [39]. Therefore, the error term $\varepsilon_{t_i}^p$ appears in (12). By denoting $\theta_4 = (\mu, \sigma, r, \sigma_c, \sigma_p)$, the

likelihood function of Model IV is

$$\begin{aligned}&L(\mathcal{D}_t^S \cup \mathcal{D}_t^C \cup \mathcal{D}_t^P|\theta_4)\\&= L(\mathcal{D}_t^S|\theta_4)\cdot L(\mathcal{D}_t^C|\theta_4, \mathcal{D}_t^S)\cdot L(\mathcal{D}_t^p|\theta_4, \mathcal{D}_t^S \cup D_t^C)\\&= L(\mathcal{D}_t^S \cup \mathcal{D}_t^C|\theta_2)\cdot \prod_{t_i\le t}\phi(P_{t_i} - C_{t_i} + S_{t_i} - Ke^{-r\tau_i})\big|\tau_i\sigma_p^2),\end{aligned}$$

where $L(\mathcal{D}_t^S \cup \mathcal{D}_t^C|\theta_2)$ is defined in (8). Thus the posterior distribution of θ_4 is obtained as

$$\begin{aligned}&p(\theta_4|\mathcal{D}_t^S \cup \mathcal{D}_t^C \cup \mathcal{D}_t^P)\\&\quad\propto \phi(\mu|\delta_\mu^2)\cdot\phi^+(\sigma|\delta_\sigma)\cdot\phi(r|\delta_r^2)\cdot\phi^+(\sigma_c|\delta_c)\\&\quad\cdot\phi^+(\sigma_p|\delta_p)\cdot L(\mathcal{D}_t^S \cup \mathcal{D}_t^C \cup \mathcal{D}_t^P|\theta_4)\end{aligned}\tag{13}$$

by setting the priors similar to Model III.

Taking advantage of the put-call parity, Model IV incorporates the dataset of put option prices without using a two-dimensional normal distribution. As a result, we avoid the complicated procedure for inferring the covariance matrix. The results in numerical experiments and empirical analysis illustrate that Model IV is much more efficient than Model III.

Remark 3: It is worth to note that we do not need to discuss the correlation between $\varepsilon_{t_i}^c$ and $\varepsilon_{t_i}^p$ in Model IV. In fact, the distribution of $\varepsilon_{t_i}^p$ is conditioned on $\varepsilon_{t_i}^c$ from the deviation of the likelihood.

E. THE DYNAMIC CALIBRATION METHOD

Inspired by the method of local volatility, parameters in the above four models are closed related to the current state of the financial market. Therefore, in order to adjust the proposed models to the current market conditions, we calibrate the parameters using the most recent data and dynamically update the dataset. To this point, we define the dynamic parameter calibration in the following definition.

Definition 1: Let θ denote the parameters to be estimated, and $\mathcal{D} = \{(t_i, x_{t_i})\}_{1\le i\le N}$ be time series dataset with $t_1 < t_2 < \cdots < t_N$ and $x_{t_i} \in \mathbb{R}^n$ can be vectors. For a fixed calibration data size n, we define the dynamic posterior distribution of θ as a family of posterior distributions $\{p(\theta|\mathcal{D}_{i,n}^*)\}_{n\le i\le N}$, where

$$\mathcal{D}_{i,n}^* = \{(t_j, x_{t_j})\}_{i-n<j\le i}.$$

Based on the dynamic posteriors, the dynamic Maximum A Posteriori Estimation (MAPE) and dynamic Expected A Posteriori Estimation (EAPE) can be respectively defined as

$$\begin{aligned}&\tilde{\theta}_i = \arg\max_{\theta\in\Theta} p(\theta|\mathcal{D}_{i,n}^*),\\&\hat{\theta}_i = \mathbb{E}\left[\theta|\mathcal{D}_{i,n}^*\right] = \int_\Theta \theta\cdot p(\theta|\mathcal{D}_{i,n}^*)\mathrm{d}\theta,\quad \forall n\le i\le N.\end{aligned}\tag{14}$$

Denote the dynamic dataset used in the above four models by

$$\begin{aligned}&\mathcal{D}_{i,n}^S = \{(t_j, S_{t_j})\}_{i-n<j\le i},\quad \mathcal{D}_{i,n}^C = \{(t_j, C_{t_j})\}_{i-n<j\le i},\\&\mathcal{D}_{i,n}^P = \{(t_j, P_{t_j})\}_{i-n<j\le i},\quad \mathcal{D}_{i,n} = \mathcal{D}_{i,n}^S \cup \mathcal{D}_{i,n}^C \cup \mathcal{D}_{i,n}^P.\end{aligned}$$

The dynamic MAPE and EAPE of the proposed four models can be easily obtained according to (14). Taking Model III as an example, for any $n \le i \le N$, the dynamic MAPE and EAPE at time t_i can be expressed as

$$\begin{aligned}&\tilde{\theta}_{3,i} = \arg\max_{\theta_3\in\Theta} p(\theta_3|\mathcal{D}_{i,n}),\\&\hat{\theta}_{3,i}^{(j)} = \mathbb{E}\left[\theta_3^{(j)}\Big|\mathcal{D}_{i,n}\right] = \int_{\Theta_j}\theta_3^{(j)}\cdot p(\theta_3^{(j)}|\mathcal{D}_{i,n})\mathrm{d}\theta_3^{(j)},\end{aligned}\tag{15}$$

for $j = 1, 2, \cdots, 6$, where $\theta_3^{(j)}$ denotes the j-th component of θ_3 and $p(\theta_3^{(j)}|\mathcal{D}_{t_i,\Delta})$ is the corresponding marginal posterior distribution. In our numerical experiments and empirical analysis, $\tilde{\theta}_{3,i}$ and $\hat{\theta}_{3,i}^{(j)}$ need to be approximated numerically because the posterior PDF is often in a complex form. More specifically, the MAPE is approximated by L-BFGS-B algorithm [40]. And the EAPE is calculated by the Monte Carlo method based on the samples from the posterior distribution by MCMC. The code in this paper is written in Python, and the MCMC sampling is implemented through the PyMC package [41].

III. NUMERICAL EXPERIMENTS

In this section, we conducted numerical experiments on the dynamic calibration of the four distinct models proposed in Section II with simulated data. Our experiments were designed to evaluate each model's performance in terms of parameter estimation accuracy and computational efficiency.

First of all, data were simulated according to the Black-Scholes model (1), (2) and Model III (10), which is the most complicated and able to generate all useful data of underlying assets, put and call options. Then a numerical test was conducted on how to select the dynamic calibration data size n. At last, we examined the efficiency and accuracy of each calibration model for a fixed n. More specifically, we calculated the errors of MAPE and EAPE, as well as the posterior standard deviation for estimations of the expected return rate μ, volatility σ and interest rate r to measure the accuracy of the parameter calibration. We selected the NUTS [35] as our MCMC sampling method in all the experiments in Section III and Section IV.

A. DATA SIMULATION

Based on Model III, we set the maturity $T = 1$ and define a uniform partition over $[0, T]$ as

$$0 = t_0 < t_1 < t_2 < \cdots < t_{N-1} < t_N = T,$$

with $N = 250$, $\Delta t = t_i - t_{i-1}$ and $t_i = i\Delta t$, for $i = 1, 2, \cdots, N$. Then we set the true values of the model parameters as follows

$$\begin{aligned}&\mu = 0.5,\quad \sigma = 1.0,\quad r = 0.2,\\&\sigma_c = 1.2,\quad \sigma_p = 1.0,\quad \rho = -0.5.\end{aligned}$$

Moreover, the call and put options are supposed to be at-the-money with the same strike price, i.e. $S_0 = K = 10.0$. The next procedure is to generate random variables according

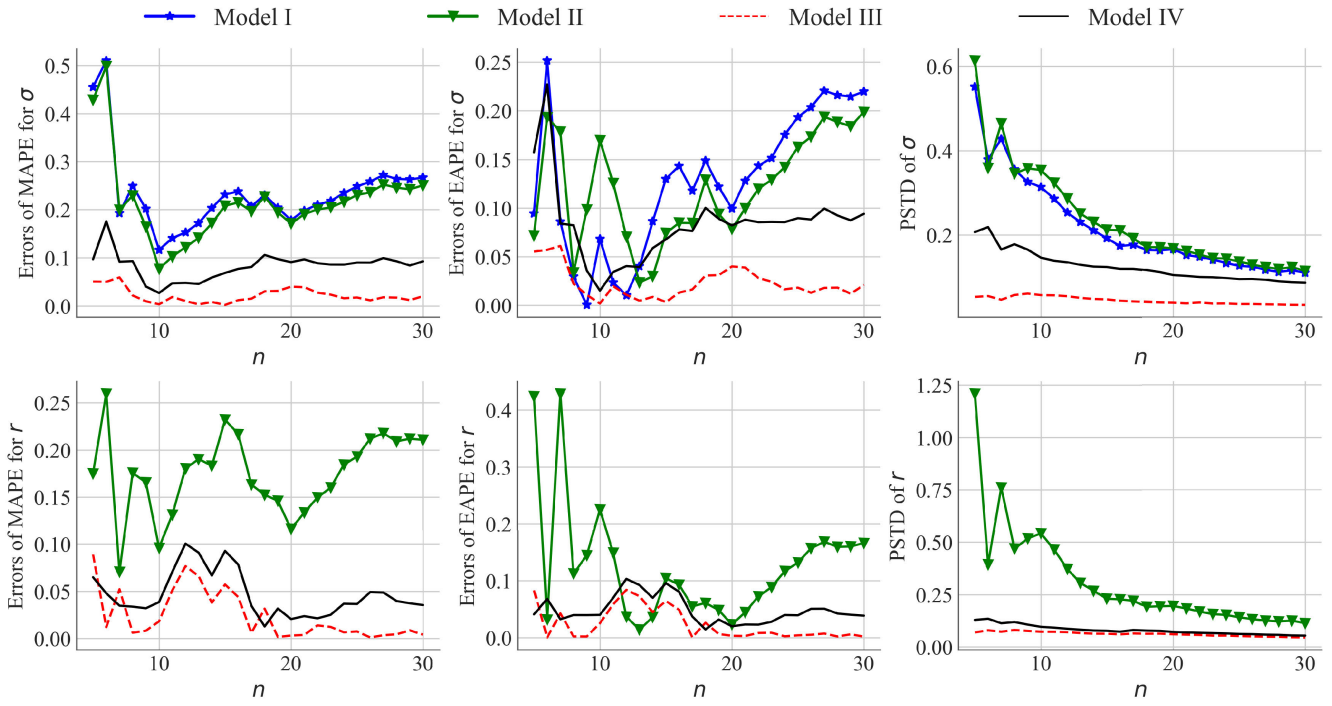

FIGURE 1. Absolute errors and the posterior standard deviation of the estimations for σ and r over different calibration data size.

to the settings of Model III. That is, for $i = 1, 2, \cdots, N$, simulate independent random numbers as

$$\Delta B_{t_i} \sim N(0, \Delta t), \quad \begin{bmatrix} \varepsilon^c_{t_i} \\ \varepsilon^p_{t_i} \end{bmatrix} \sim N\left(0, \tau_i \begin{bmatrix} \sigma_c^2 & \rho\sigma_c\sigma_p \\ \rho\sigma_c\sigma_p & \sigma_p^2 \end{bmatrix}\right), \tag{16}$$

where $\Delta B_{t_i} = B_{t_i} - B_{t_{i-1}}$, $\tau_i = T - t_i$. Then we compute the prices of underlying assets, put and call options as

$$\begin{aligned} S_{t_i} &= S_0 \exp\left((\mu - \frac{1}{2}\sigma^2)t_i + \sigma B_{t_i}\right), \\ C_{t_i} &= \hat{C}(t_i, S_{t_i}) + \varepsilon^c_{t_i}, \\ P_{t_i} &= \hat{P}(t_i, S_{t_i}) + \varepsilon^p_{t_i}, \end{aligned}$$

where $B_{t_i} = \sum_{j=1}^{i} \Delta B_{t_j}$, $\hat{C}(t_i, S_{t_i})$ and $\hat{P}(t_i, S_{t_i})$ are defined in (2). Thus we generate all the necessary datasets for the dynamic calibration.

B. ANALYSIS OF CALIBRATION DATA SIZE

In this section, we analyze the impact of varying calibration data size n on the accuracy of parameter estimation in the proposed four models. We assess the errors in both volatility and interest rate estimations, which are crucial in option pricing, using MAPE and EAPE techniques. The posterior standard deviation (PSTD) are also analyzed. As an illustration, we set $i = 100$ and plot our results over different data size n in Figure 1.

The results show that the absolute errors and PSTD of Model III and Model IV are much smaller than the other two models for almost every n. Moreover, as more data are included in the parameter calibration, the accuracy and stability for each model are improved gradually. Particularly when $n \geq 20$, the errors and standard deviations become small and stable. Therefore, in the following studies, we set the dynamic calibration data size $n = 20$.

C. ANALYSIS OF THE RUNNING TIMES

To compare the efficiency of the four models, we examined their running times with the same setting $n = 20$. In the process of calculating EAPE, the most important step is to get samples from MCMC sampling. While the main procedure in obtaining MAPE is to find the maxima of the posterior by the optimization method iteratively. The running times of calculating EAPE and MAPE are presented in Figure 2.

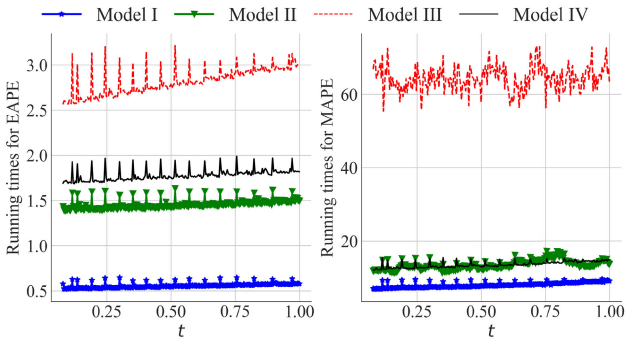

FIGURE 2. Running times of calculating EAPE and MAPE by the four distinct models.

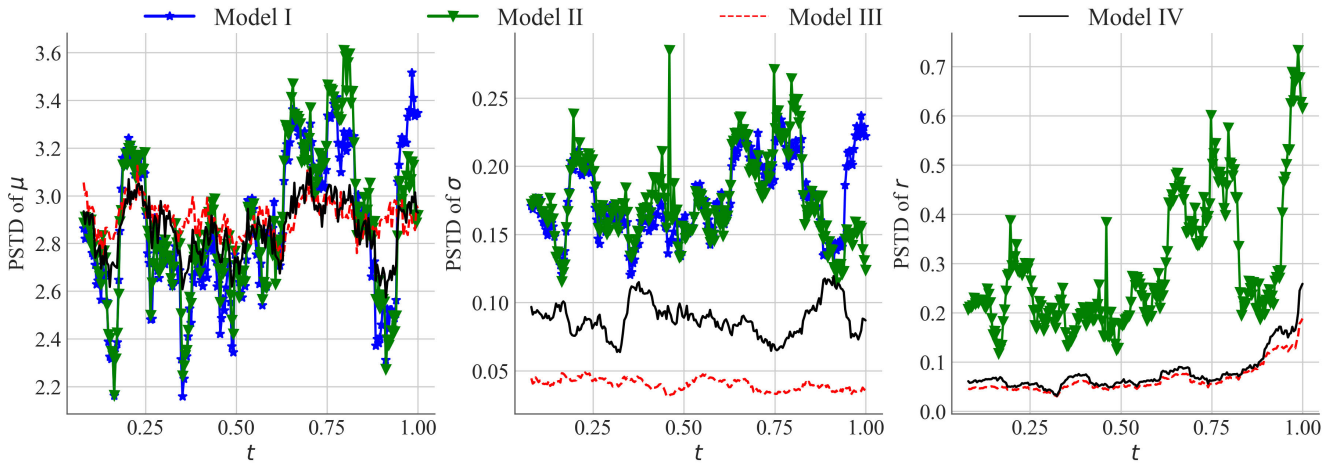

FIGURE 3. PSTD for μ, σ and r by dynamic calibration with $n = 20$.

It is obvious from the above figure that the computational complexity of Model III is significantly higher than that of the other models. Model IV greatly simplifies Model III by using the put-call parity, reducing its model complexity to be on the same level as that of Model I and Model II.

D. ANALYSIS OF THE ACCURACY

The next experiments focus on testing the calibration accuracy of the four distinct models. The primary discussion is on the accuracy for μ, σ and r. As mentioned above, σ and r are key parameters in option pricing. Although the expected return rate μ does not appear directly in the option pricing formula, it influences the changes in the price of the underlying asset, which in turn affects predictions of option prices.

In this section, we calculated the root mean squared error (RMSE) for MAPE and EAPE, and compared the standard deviation of the estimated posterior distributions. The corresponding results are presented in Table 2 and Figure 3.

TABLE 2. RMSE of dynamic calibration for μ, σ and r with $n = 20$.

Model	RMSE of μ		RMSE of σ		RMSE of r	
	MAPE	EAPE	MAPE	EAPE	MAPE	EAPE
I	1.84e+00	1.76e+00	1.84e-01	1.62e-01	-	-
II	1.82e+00	1.73e+00	1.83e-01	1.62e-01	2.36e-01	2.66e-01
III	1.66e+00	1.66e+00	3.50e-02	3.54e-02	7.40e-02	7.48e-02
IV	1.71e+00	1.72e+00	6.97e-02	6.98e-02	1.01e-01	1.01e-01

For the considered three parameters, the experimental results in Table 2 show that the calibration accuracy for σ and r is much more accurate than μ. And the calibration errors for μ is similar over the four models. This is because, although the subsequent models increase in complexity and dataset, the data containing information on the expected return is limited to the price of the underlying asset, which has been already fully incorporated in Model I.

For the four distinct models, it is clear from the errors listed in Table 2 that calibration based on Model III has the highest accuracy for all considered parameters. The calibration errors of Model IV is slightly larger than that of Model III. But they are essentially on the same level and significantly better than the estimation results of Model I and Model II. The PSTD shown in Figure 3 also confirms that the dynamic calibration procedure based on Model III and IV are more accurate and stable than Model I and II.

Therefore, through the above results of numerical experiments, we have arrived at the following conclusions: Model III and IV significantly improve the accuracy of calibration by introducing more data. Although there is no large enhancement for the calibration accuracy of μ, the fluctuations of PSTD obtained by Model III and IV are much less, which implies a better stability. Additionally, Model IV greatly reduces the computational complexity by utilizing the put-call parity, making the parameter calibration more efficient. In summary, Models III and IV are significantly superior to Model I and Model II in the proposed dynamic calibration procedure. Therefore, in the empirical analysis, we mainly discuss the empirical results of Model III and Model IV, with Model I and Model II only appearing as references for comparison.

IV. EMPIRICAL ANALYSIS OF SPX OPTIONS

In this section, we employed the European option data on the Standard & Poor's 500 Index (SPX) with the same maturity date on 8th September, 2023 and different strike prices ranges from 3500 to 4500, covering the 245 trading days from 16th September, 2022 to 8th September, 2023. Time in our dataset is expressed in years, so that the length of each day is set to be $1/365$. In case there is no deals on some trading days, the midpoint between bid and ask prices is used as the price

TABLE 3. Convergence diagnostics of MCMC sampling by global and dynamic calibration based on Model III. Small Monte Carlo standard errors for mean (MCSE Mean) and standard deviation (MCSE SD) and large effective sample size (ESS) are observed, as well as the value of $\hat{R}$ closed to 1.

	Global calibration					Dynamic calibration ($i = 133$)				
	MCSE Mean	MCSE SD	ESS Bulk	ESS Tail	$\hat{R}$	MCSE Mean	MCSE SD	ESS Bulk	ESS tail	$\hat{R}$
μ	0.0019	0.0016	12304	8318	1.0004	0.0072	0.0063	9354	6544	1.0009
σ	0.0000	0.0000	10318	7568	1.0003	0.0000	0.0000	8977	5755	1.0004
r	0.0000	0.0000	12629	8619	0.9998	0.0000	0.0000	8875	6514	1.0000

data. All data in this paper are sourced from the Bloomberg database.

To illustrate the advantages of dynamic calibration, we introduce a global calibration method for comparison. Recalling the Definition 1, global calibration means the posterior distribution, MAPE and EAPE are obtained based on the entire dataset $\mathcal{D}$, which means more data are exploited while the dynamic property of parameters is overlooked.

This section contains three parts. First of all, a comparison was made between the global and dynamic calibration on the accuracy of data fitting and option pricing. Then we attempted to predict option prices by the dynamic calibration method under the condition that the price of underlying asset is unknown. Highest posterior density intervals (HPDI) are estimated by using the proposed four models. In the end, we investigated other properties of dynamic calibration. The volatility surface was computed and the leptokutic property of log returns was reproduced.

A. COMPARISON BETWEEN GLOBAL AND DYNAMIC CALIBRATION

In this section, we compare the accuracy of global and dynamic calibration on the option data with strike price $K = 4000$ based on Model III and Model IV. Firstly, we conducted convergence diagnostics for the MCMC sampling because it is crucial for our approximations on posterior distribution and EAPE. For each estimation in our experiments, four Markov chains are generated at the same time. After discarding the first 1000 samples in each chain, the subsequent 2500 samples are selected to ensure the convergence, making a total of 10000 samples.

In Table 3, we listed the main results of the MCMC sampling for global and dynamic calibration based on Model III, which is the most complicated. For the dynamic calibration, we only listed the results on the dataset $\mathcal{D}_{i,n}$ with $i = 133$ and $n = 20$. The results clearly indicate that the Markov chains has reached their stationary distribution for both global and dynamic calibrations. The corresponding results computed by Model IV is very similar, so they are not listed here. Consequently, in the data fitting part, we just take Model III as an example. And in the option pricing part, only the results of Model IV are provided.

1) DATA FITTING

This section compares global and dynamic calibration methods in terms of data fitting for call and put options. First of all, the results of calibration for key parameters in option pricing by Model III are shown in Table 4 and Figure 4.

TABLE 4. Results of the global calibration by Model III.

Parameters	Global calibration			
	MAPE	EAPE	PSTD	50% HPDI
μ	0.1738	0.1745	0.2093	(0.0293, 0.3113)
σ	0.2106	0.2107	0.0009	(0.2101, 0.2113)
r	0.0334	0.0334	0.0004	(0.0332, 0.0337)

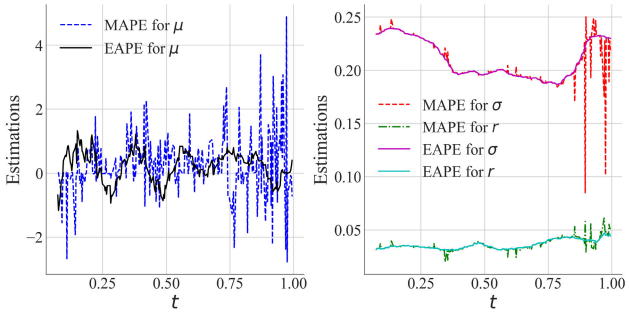

FIGURE 4. Results of dynamic calibration for μ, σ and r by Model III.

From the results, it is evident that the calibration accuracy for μ is significantly lower than that for σ and r in both global and dynamic calibration. But this part focuses on option prices, which is theoretically irrelevant to μ in data fitting and option pricing. In the dynamic calibration, EAPE has less fluctuation and is more stable than MAPE, especially near the expiration date. But during this period, the primary impact on option prices is the underlying asset price. The effects of volatility and interest rate diminish, which will not lead to significant fluctuations in option prices.

Remark 4: The severe fluctuations of MAPE near expiration date are due to the oscillations of optimization algorithm. The reasons for this phenomenon are twofold. On the one hand, the complex structure of Model III makes it more difficult for the optimization algorithm to find the maximum value point. On the other hand, the gradient of the option price function with respect to the estimated parameters is very close to zero near the expiration date, which further increases the difficulty of the optimization process.

With the results of global and dynamic calibration, the estimated put and call option prices can be calculated by the

Black-Scholes formula (2), that is

$$\begin{aligned}
\tilde{C}^G_{t_i} &= \hat{C}(t_i, S_{t_i}; \tilde{\sigma}, \tilde{r}), \quad \tilde{P}^G_{t_i} = \hat{P}(t_i, S_{t_i}; \tilde{\sigma}, \tilde{r}),\\
\hat{C}^G_{t_i} &= \hat{C}(t_i, S_{t_i}; \hat{\sigma}, \hat{r}), \quad \hat{P}^G_{t_i} = \hat{P}(t_i, S_{t_i}; \hat{\sigma}, \hat{r}),\\
\tilde{C}^D_{t_i} &= \hat{C}(t_i, S_{t_i}; \tilde{\sigma}_i, \tilde{r}_i), \quad \tilde{P}^D_{t_i} = \hat{P}(t_i, S_{t_i}; \tilde{\sigma}_i, \tilde{r}_i),\\
\hat{C}^D_{t_i} &= \hat{C}(t_i, S_{t_i}; \hat{\sigma}_i, \hat{r}_i), \quad \hat{P}^D_{t_i} = \hat{P}(t_i, S_{t_i}; \hat{\sigma}_i, \hat{r}_i), \qquad (17)
\end{aligned}$$

where $\tilde{C}^G_{t_i}$ and $\hat{C}^G_{t_i}$ are the estimated prices of call options at time t_i based on MAPE $(\tilde{\sigma}, \tilde{r})$ and EAPE $(\hat{\sigma}, \hat{r})$ by global calibration, $\tilde{C}^D_{t_i}$ and $\hat{C}^D_{t_i}$ are the estimated prices of call options at time t_i based on MAPE $(\tilde{\sigma}_i, \tilde{r}_i)$ and EAPE $(\hat{\sigma}_i, \hat{r}_i)$ by dynamic calibration, respectively, $\tilde{P}^G_{t_i}, \hat{P}^G_{t_i}, \tilde{P}^D_{t_i}, \hat{P}^D_{t_i}$ are the corresponding estimated put option prices.

It is worth to note that S_{t_i} is the price at time t_i from the real market, so the comparison between prices defined in (17) and in the real market is to examine the performance of data fitting. The relative errors are shown in Figure 5 and Figure 6.

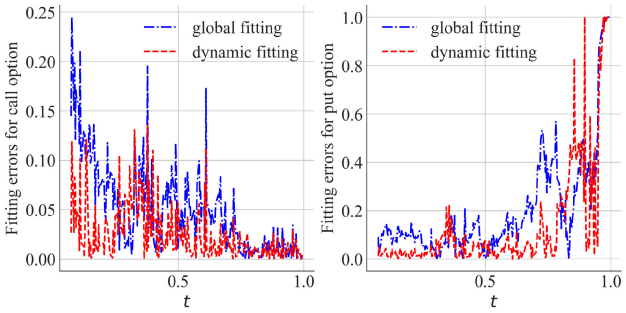

FIGURE 5. Relative errors of data fitting using MAPE.

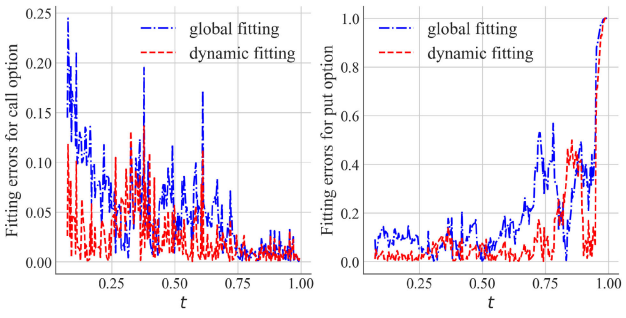

FIGURE 6. Relative errors of data fitting using EAPE.

From above figures, we can see the relative errors of dynamic fitting is smaller than global fitting in general for both call and put options, except that the fitting error for put option prices rapidly increases near the expiration date. That is because put options are deeply out of the money in this period, and the market price approaches zero.

2) OPTION PRICING

In this section, we test the accuracy of dynamic calibration based on Model IV in terms of option pricing. Firstly, we clarify the option pricing problem under consideration here. Given a fixed time t_i, suppose the data of underlying asset, call and put options before t_i are available. Then for t_{i+k}, pricing the call and put options under the condition that $S_{t_{i+k}}$ is known with k being a positive integer. Thus we define

$$\begin{aligned}
\tilde{\mathcal{C}}_{t_{i+k}} &= \hat{C}(t_{i+k}, S_{t_{i+k}}; \tilde{\sigma}_i, \tilde{r}_i), \tilde{\mathcal{P}}_{t_{i+k}} = \hat{P}(t_{i+k}, S_{i+k}; \tilde{\sigma}_i, \tilde{r}_i),\\
\hat{\mathcal{C}}_{t_{i+k}} &= \hat{C}(t_{i+k}, S_{t_{i+k}}; \hat{\sigma}_i, \hat{r}_i), \hat{\mathcal{P}}_{t_{i+k}} = \hat{P}(t_{i+k}, S_{t_{i+k}}; \hat{\sigma}_i, \hat{r}_i),
\end{aligned}$$

where $\tilde{\mathcal{C}}_{t_{i+k}}$ and $\hat{\mathcal{C}}_{t_{i+k}}$ are call option pricing at t_{i+k} by the MAPE and EAPE of dynamic calibration respectively, $\tilde{\mathcal{P}}_{t_{i+k}}$ and $\hat{\mathcal{P}}_{t_{i+k}}$ are the corresponding prices of put option pricing. We only define the notations for option pricing with dynamic calibration, because the option pricing with global calibration is the same to the data fitting. That is to say, the call option pricing at time t_{i+k} based on MAPE by global calibration is $\hat{C}(t_{i+k}, S_{t_{i+k}}; \tilde{\sigma}, \tilde{r}) = \tilde{C}^G_{t_{i+k}}$ according to (17).

To illustrate the relative errors of option pricing over a period to time, we define the root mean square relative errors (RMSRE). As an example, for a given k, the RMSRE of option pricing by MAPE of dynamic calibration over the period $[t_{n+k}, t_N]$ is defined as

$$\tilde{\varepsilon}^D_{RMSRE} = \sqrt{\frac{1}{N-k-n+1}\sum_{i=n}^{N-k}\left(\frac{\tilde{\mathcal{C}}_{t_{i+k}} - C_{t_{i+k}}}{C_{t_{i+k}}}\right)^2}.$$

Then the RMSREs based on MAPE and EAPE of global and dynamic calibration are listed in Table 5, from which we can easily see that dynamic calibration is more accurate than global calibration in option pricing.

TABLE 5. RMSREs of the k-day option pricing by global and dynamic calibration for $k = 1, 2, \cdots, 5$.

k	Type	Global calibration		Dynamic calibration	
		MAPE	EAPE	MAPE	EAPE
$k=1$	Call	1.6327e-01	1.6667e-01	3.7449e-02	3.7420e-02
	Put	4.0325e-01	4.0837e-01	2.7366e-01	2.6198e-01
$k=2$	Call	7.2622e-02	7.2613e-02	3.7881e-02	3.7834e-02
	Put	2.8836e-01	2.8838e-01	2.7570e-01	2.6376e-01
$k=3$	Call	7.2566e-02	7.2558e-02	3.9135e-02	3.9093e-02
	Put	2.8885e-01	2.8886e-01	2.7871e-01	2.6695e-01
$k=4$	Call	7.1553e-02	7.1545e-02	4.0049e-02	4.0025e-02
	Put	2.8943e-01	2.8945e-01	2.8216e-01	2.7027e-01
$k=5$	Call	7.1279e-02	7.1272e-02	4.1429e-02	4.1436e-02
	Put	2.8996e-01	2.8998e-01	2.8564e-01	2.7384e-01

The main reason of the better results for dynamic calibration is that the dynamic estimates of model parameters vary over time, which reflects the current state of market more precisely. The global estimates of parameters are only constant values, which only reflect the mean state of the market and lead to greater errors.

B. OPTION PRICE PREDICTION

In this section, we focuses on examining the accuracy of price prediction for call and put options. Different from

TABLE 6. Comparison of price prediction accuracy for call and put options by dynamic calibration based on all models.

k		Model I		Model II		Model III		Model IV	
		Call	Put	Call	Put	Call	Put	Call	Put
$k=1$	Inside Percent	0.635	0.457	0.896	0.348	0.721	0.557	0.726	0.600
	50% HPDI size	109.726	75.558	114.086	111.25	63.9936	27.835	64.778	29.704
	Ratio	0.0058	0.0060	0.0079	0.0036	0.0113	0.0200	0.0112	0.0201
$k=2$	Inside Percent	0.690	0.515	0.904	0.402	0.755	0.629	0.755	0.655
	50% HPDI size	141.327	89.054	146.216	111.247	98.056	42.217	98.360	44.040
	Ratio	0.0049	0.0057	0.0061	0.0036	0.0077	0.0150	0.0076	0.0149
$k=3$	Inside Percent	0.741	0.531	0.899	0.496	0.766	0.675	0.771	0.684
	50% HPDI size	168.119	100.367	173.764	125.274	126.985	54.342	127.033	56.127
	Ratio	0.0044	0.0053	0.0051	0.0040	0.0060	0.0124	0.0061	0.0121
$k=4$	Inside Percent	0.753	0.551	0.885	0.577	0.824	0.705	0.833	0.718
	50% HPDI size	192.714	110.607	198.964	137.861	153.382	65.289	153.290	67.031
	Ratio	0.0039	0.0049	0.0045	0.0041	0.0053	0.0108	0.0054	0.0107
$k=5$	Inside Percent	0.770	0.553	0.894	0.624	0.827	0.726	0.827	0.735
	50% HPDI size	215.607	120.099	222.500	149.550	177.8200	75.458	177.783	77.1606
	Ratio	0.0035	0.0046	0.0040	0.0042	0.0047	0.0096	0.0047	0.0095

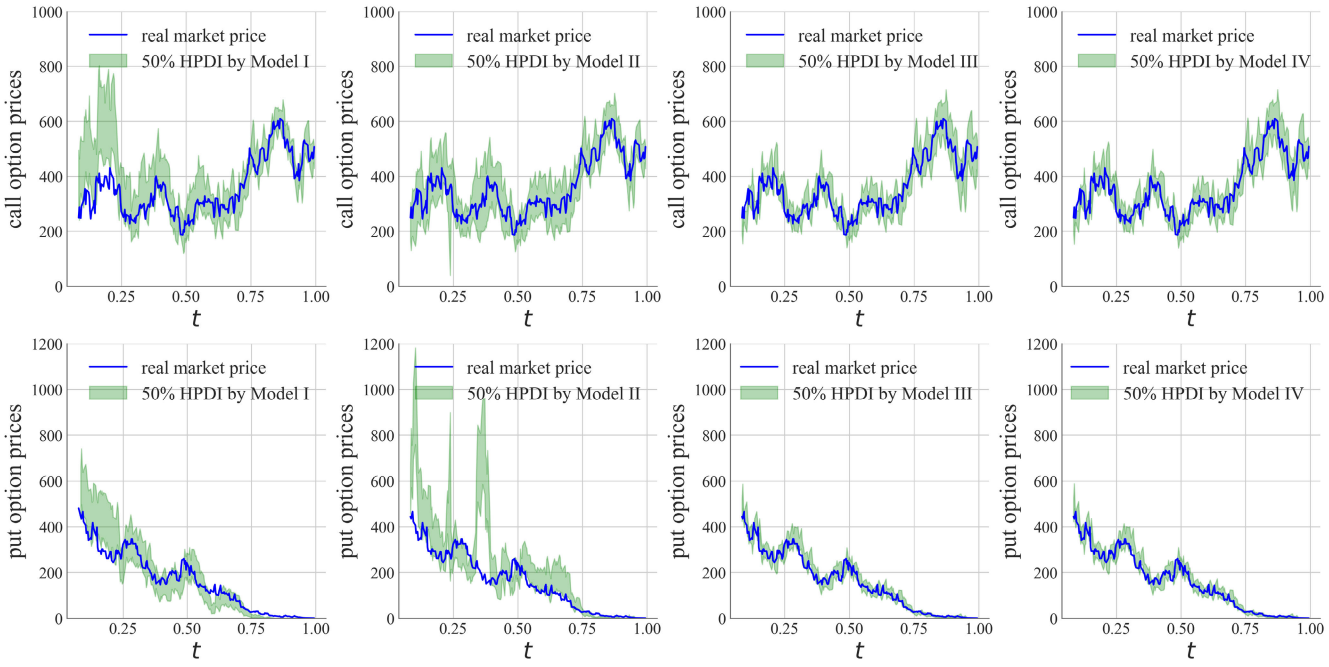

FIGURE 7. 50% HPDI of price prediction for call (top) and put (bottom) options obtained by dynamic calibration based on all models for $k = 2$.

the option pricing, the price of the underlying asset $S_{t_{i+k}}$ is assumed to be unknown in price prediction. As a result, option price prediction consists of two steps: firstly, predict the price of the underlying asset by the SDE (1); secondly, predict the price of the option by the predicted price of the underlying asset and the calibrated parameters. In fact, it is challenging to find a point estimation for the price prediction of the underlying asset. Because the solution of SDE (1) is influenced by the trajectory of the Brownian motion, which is stochastic. Therefore, we conduct interval estimations for option price predictions, which means computing the highest posterior density interval (HPDI) for predictions of option price. Moreover, in the global calibration, all the available data have already been used including the spot and option prices we need to predict. So we just compare the accuracy among the four different models by dynamic calibration.

To express the details, let $\{(\mu_i^{(m)}, \sigma_i^{(m)}, r_i^{(m)})\}_{m=1}^{M}$ be the MCMC samples from the dynamic calibration at time t_i. And $\{\xi^{(l)}\}_{l=1}^{L}$ be a sequence of random numbers following standard normal distribution. Then for each sample, we predict

the price of underlying asset at t_{i+k} by

$$S_{t_{i+k}}^{(m,l)} = S_{t_i} \exp\left((\mu_i^{(m)} - \frac{1}{2}(\sigma_i^{(m)})^2)\Delta t_{i,k} + \sigma_i^{(m)}\sqrt{\Delta t_{i,k}}\xi^{(l)}\right),$$

for $m = 1, 2, \cdots, M$ and $l = 1, 2, \cdots, L$, where $\Delta t_{i,k} = t_{i+k} - t_i$. Then the predicted prices of call and put options can be computed for all m and l by

$$C_{t_{i+k}}^{(m,l)} = \hat{C}(t_{i+k}, S_{t_{i+k}}^{(m,l)}; \sigma_i^{(m)}, r_i^{(m)}),$$
$$P_{t_{i+k}}^{(m,l)} = \hat{P}(t_{i+k}, S_{t_{i+k}}^{(m,l)}; \sigma_i^{(m)}, r_i^{(m)}).$$

Finally, for a given probability p, find the $\alpha = \frac{1-p}{2}$ and $\beta = \frac{1+p}{2}$ quantiles of the samples $\{C_{t_{i+k}}^{(m,l)}\}$ and $\{P_{t_{i+k}}^{(m,l)}\}$, which is denoted by $C_{t_{i+k}}^{\alpha}$, $C_{t_{i+k}}^{\beta}$ and $P_{t_{i+k}}^{\alpha}$, $P_{t_{i+k}}^{\beta}$, respectively. Thus the HPDI with probability p for the predictions of call and put option prices are $[C_{t_{i+k}}^{\alpha}, C_{t_{i+k}}^{\beta}]$ and $[P_{t_{i+k}}^{\alpha}, P_{t_{i+k}}^{\beta}]$.

Remark 5: The parameters in Model I do not include the interest rate r. So we use the federal funds rate and the cubic spline of the yield curve as our reference data.

In our following analysis, we set $p = 0.5$ and compute the k-day prediction HDPI for $i = n, \cdots, N - k$ based on four proposed models by dynamic calibration for $k = 1, 2, \cdots, 5$. Then we calculate the percentage of real data falling inside the 50% HPDI and the average size of the prediction interval, which is listed in Table 6.

The calculation results indicate that Model III and Model IV have a better accuracy on the price prediction than Model I and Model II. Because the size of HPDI in Model III and Model IV are smaller, and their inside percentage are higher for both call and put options. When k increases, the ratio of inside percentage to interval size becomes small for all models, which means the prediction accuracy is decreasing. The main reason for this phenomenon is that the estimation of μ in dynamic calibration is of relatively low accuracy, leading to a decrease in the prediction accuracy of the underlying asset price as the length of time interval becomes larger. To further illustrate the prediction accuracy, we plot the market prices and 50% HPDI obtained by the proposed four models for $k = 2$ in Figure 7.

C. OTHER PROPERTIES OF DYNAMIC CALIBRATION

Although the proposed four models in this paper are all based on the classic the Black-Scholes framework, the dynamic calibration method enables them to possess many fine properties. To illustrate these properties more clearly, we analyze the dynamic calibration methods from two aspects: the volatility surface and the log returns of the underlying asset.

1) VOLATILITY SURFACE

Firstly, we draw the volatility surface by the dynamic calibration method based on Model III, as an example. Different from the standard volatility surface, which serves as a graphical representation of implied volatility across a range of strike prices and expiration dates, we calculate the volatility of a set of options with different strike prices but the same expiration date T by dynamic calibration method from $t \in [0, T]$. Moreover, the calibrated volatility is not just implied because the historical data of options and underlying asset are used together.

According to the price of the S&P 500 index, we selected 22 options with the expiration date of 15th September, 2023, including 11 call options and 11 put options with strike prices ranging from 3500 to 4500 with an interval of 100. Then the volatility of each option is calibrated by dynamic method based Model III from 16th September, 2022 to 8th September, 2023. The results are shown in Figure 8.

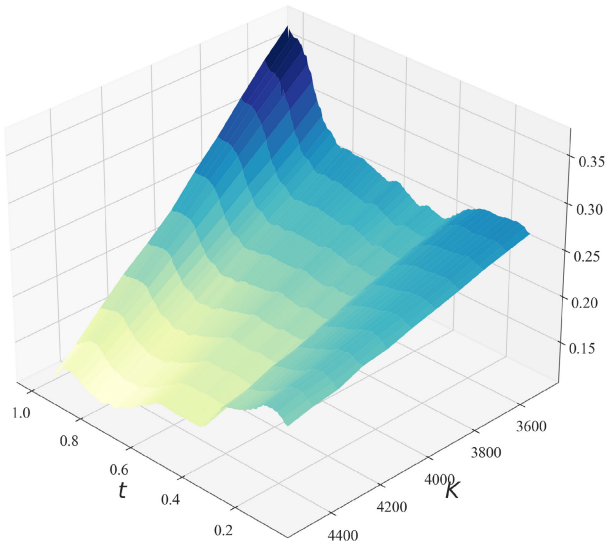

FIGURE 8. Volatility surface estimated MAPE obtained by dynamic calibration based on Model III.

From the figure, it is clearly that the calibrated volatility changes over time. And there is a distinct skewness in the volatility for different strike prices on each day, which is consistent with the theoretical results for SPX options.

2) LEPTOKURTIC PROPERTY

One of the main drawbacks of the Black-Scholes model is the assumption that the log returns of the underlying asset follow a normal distribution, which is actually derived from the assumption of a constant expected return and volatility. Fortunately, the dynamic calibration method is able to approximate μ and σ with a time-varying estimation, which makes it possible for the log returns of the underlying asset to exhibit the leptokurtic property in the calibrated model, which is consistent with the data from real markets. To this end, regenerate the log returns of the SPX with μ and σ calibrated by the dynamic method based on Model IV according to the following equations,

$$\tilde{R}_i = \log\left(\frac{S_{t_{i+1}}}{S_{t_i}}\right) = (\tilde{\mu}_i - \frac{1}{2}\tilde{\sigma}_i^2)\Delta t_i + \tilde{\sigma}_i \Delta B_{t_i}, \quad (18)$$

$$\hat{R}_i = \log\left(\frac{S_{t_{i+1}}}{S_{t_i}}\right) = (\hat{\mu}_i - \frac{1}{2}\hat{\sigma}_i^2)\Delta t_i + \hat{\sigma}_i \Delta B_{t_i}, \quad (19)$$

where $\Delta B_{t_i} \sim N(0, \Delta t_i)$, and $(\tilde{\mu}_i, \tilde{\sigma}_i)$ and $(\hat{\mu}_i, \hat{\sigma}_i)$ are MAPE and EAPE for expected return and volatility by dynamic calibration with data size $n = 20$, respectively. Then the basic statistics for $\{\tilde{R}_i\}_{i=1}^N$ and $\{\hat{R}_i\}_{i=1}^N$ are listed in Table 7. To make it more clear, we draw the histogram of the generated data and the corresponding probability density function of normal distribution for comparison in Figure 9.

TABLE 7. Basic statistics for the regenerated log returns.

Data	Estimation	Mean	Variance	Skewness	Kurtosis
$\{\tilde{R}_i\}_{i=1}^N$	MAPE	0.0115	0.0011	-0.2215	4.2558
$\{\hat{R}_i\}_{i=1}^N$	EAPE	0.0115	0.0011	-0.1929	4.1415

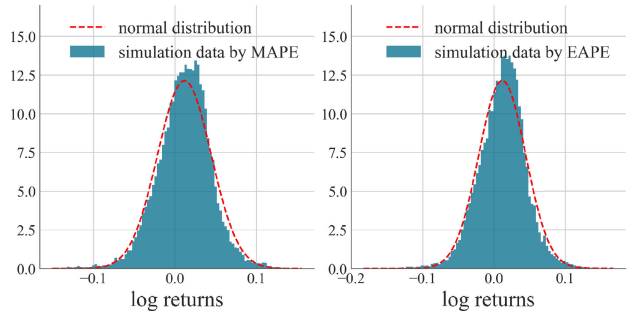

FIGURE 9. Comparison between the regenerated data by MAPE (left) and EAPE (right) based on Model IV and the Normal distribution.

From the statistics in Table 7 and Figure 9, it is clearly evident that the distribution of the regenerated log returns exhibits the features of leptokurtosis and negative skewness. In fact, many researches have focused on improving the Black-Scholes model by assuming the log returns of the underlying asset follow a leptokurtic distribution, which has made the option pricing model increasingly complex and the calibration of parameters more difficult. The dynamic calibration method proposed in this paper achieves this goal without increasing the complexity of the model, which improved the standard Black-Scholes model in a highly efficient manner.

V. CONCLUSION

In conclusion, our study has provided comprehensive insights into the accuracy and efficiency of dynamic calibration by Bayesian method based on the Black-Scholes model. The proposed dynamic calibration method has a better performance than the global calibration method in terms of data fitting, option pricing, and option price prediction. Among the four proposed calibration models, Model III and Model IV exhibit better performance than other models. More specifically, Model III has the highest accuracy, while Model IV is more efficient. In addition, the log returns of underlying asset exhibit leptokurtic and negative skew features in the dynamically calibrated Black-Scholes model, which is a significant improvement over the classic Black-Scholes model, making it more consistent with market data without introducing new complex models.

The reasons why dynamic calibration with Model III and Model IV have better performances are twofold. First of all, the calibrated parameters by dynamic calibration change over time, making them more responsive to changes in market states. Secondly, different types of the data allow for a certain degree of accuracy in parameter estimation.

Besides the aforementioned advantages, to improve the accuracy of option price prediction by the proposed dynamic calibration method still requires a more precise estimation on the expected return rate μ. However, it is difficult to simply improve the accuracy of estimating μ following the method of this paper. Because adding information on the option prices will not help. In fact, the expected return rate influences the prediction of the spot price, which significantly affects the accuracy of option price prediction. Therefore, from a more general perspective, we should focus on the accuracy of predicting the price of the underlying asset, rather than just concerning with obtaining a more precise estimation on μ. To this point, many improvements could be made for the spot price prediction model. For example, Long Short-Term Memory (LSTM), deep learning models, and so on. A major feature of these models is that they exploit more information from the spot market, such as opening prices, closing prices and trading volumes, which can make the prediction of the underlying asset prices more accurate. Moreover, our future work also includes finding applications of dynamic calibration method in American option and exotic option pricing models.

ACKNOWLEDGMENT

The authors would like to thank the developers of the PyMC Python library, which helps them a lot in establishing Bayesian models and conducting MCMC sampling.

REFERENCES

[1] F. Black and M. Scholes, "The pricing of options and corporate liabilities," *J. Political Economy*, vol. 81, no. 3, pp. 637–654, May 1973.
[2] S. G. Kou, "A jump-diffusion model for option pricing," *Manage. Sci.*, vol. 48, no. 8, pp. 1086–1101, Aug. 2002.
[3] S. L. Heston, "A closed-form solution for options with stochastic volatility with applications to bond and currency options," *Rev. Financial Stud.*, vol. 6, no. 2, pp. 327–343, Apr. 1993.
[4] B. Dupire, "Pricing with a smile," *Risk*, vol. 7, no. 1, pp. 18–20, 1994.
[5] P. Hagan, A. Lesniewski, and D. Woodward, "Probability distribution in the SABR model of stochastic volatility," in *Large Deviations and Asymptotic Methods in Finance*. Cham, Switzerland: Springer, 2015, pp. 1–35.
[6] Z. Cui, J. L. Kirkby, and D. Nguyen, "A general valuation framework for SABR and stochastic local volatility models," *SIAM J. Financial Math.*, vol. 9, no. 2, pp. 520–563, Jan. 2018.
[7] D. Duffie, J. Pan, and K. Singleton, "Transform analysis and asset pricing for affine jump-diffusions," *Econometrica*, vol. 68, no. 6, pp. 1343–1376, Nov. 2000.
[8] R. Cont and P. Tankov, *Financial Modelling With Jump Processes* (Financial Mathematics Series). Boca Raton, FL, USA: Chapman & Hall, 2004.
[9] J. Duan, "The GARCH option pricing model," *Math. Finance*, vol. 5, no. 1, pp. 13–32, Jan. 1995.
[10] H. Nie and H. Waelbroeck, "Coupled GARCH(1,1) model," *Quant. Finance*, vol. 23, no. 5, pp. 759–776, May 2023.

[11] C. Bayer, P. Friz, and J. Gatheral, "Pricing under rough volatility," *Quant. Finance*, vol. 16, no. 6, pp. 887–904, Jun. 2016.
[12] M. Forde and H. Zhang, "Asymptotics for rough stochastic volatility models," *SIAM J. Financial Math.*, vol. 8, no. 1, pp. 114–145, Jan. 2017.
[13] S. N. Cohen, C. Reisinger, and S. Wang, "Arbitrage-free neural-SDE market models," *Appl. Math. Finance*, vol. 30, no. 1, pp. 1–46, Jan. 2023.
[14] I. P. Arribas, C. Salvi, and L. Szpruch, "Sig-SDEs model for quantitative finance," in *Proc. 1st ACM Int. Conf. AI Finance*. New York, NY, USA: Association for Computing Machinery, Oct. 2020, pp. 1–15.
[15] C. Cuchiero, G. Gazzani, and S. Svaluto-Ferro, "Signature-based models: Theory and calibration," *SIAM J. Financial Math.*, vol. 14, no. 3, pp. 910–957, Sep. 2023.
[16] F. Mariani, G. Pacelli, and F. Zirilli, "Maximum likelihood estimation of the Heston stochastic volatility model using asset and option prices: An application of nonlinear filtering theory," *Optim. Lett.*, vol. 2, no. 2, pp. 177–222, Mar. 2008.
[17] C. L. Yu, H. Li, and M. T. Wells, "MCMC estimation of Lévy jump models using stock and option prices," *Math. Finance*, vol. 21, no. 3, pp. 383–422, Jul. 2011.
[18] A. Luoma, A. Puustelli, and L. Koskinen, "Bayesian analysis of equity-linked savings contracts with American-style options," *Quant. Finance*, vol. 14, no. 2, pp. 343–356, Feb. 2014.
[19] R. Gao, Y. Li, and Y. Bai, "Numerical pricing of exchange option with stock liquidity under Bayesian statistical method," *Commun. Statist. Theory Methods*, vol. 51, no. 10, pp. 3312–3333, May 2022.
[20] S. Crépey, "Calibration of the local volatility in a generalized black–scholes model using Tikhonov regularization," *SIAM J. Math. Anal.*, vol. 34, no. 5, pp. 1183–1206, Jan. 2003.
[21] J. Geng, I. M. Navon, and X. Chen, "Non-parametric calibration of the local volatility surface for European options using a second-order Tikhonov regularization," *Quant. Finance*, vol. 14, no. 1, pp. 73–85, Jan. 2014.
[22] V. V. L. Albani and J. P. Zubelli, "A splitting strategy for the calibration of jump-diffusion models," *Finance Stochastics*, vol. 24, no. 3, pp. 677–722, Jul. 2020.
[23] M. Avellaneda, C. Friedman, R. Holmes, and D. Samperi, "Calibrating volatility surfaces via relative-entropy minimization," *Appl. Math. Finance*, vol. 4, no. 1, pp. 37–64, Mar. 1997.
[24] R. Cont and P. Tankov, "Nonparametric calibration of jump-diffusion option pricing models," *J. Comput. Finance*, vol. 7, pp. 1–49, Aug. 2004.
[25] C. C. Xu and Z. L. Xu, "Option pricing method and parameter calibration for jump-diffusion model," *Acta Math. Sci. Ser. A Chin. Ed.*, vol. 39, no. 3, pp. 649–663, 2019.
[26] B. Engelmann, F. Koster, and D. Oeltz, "Calibration of the Heston stochastic local volatility model: A finite volume scheme," *Int. J. Financial Eng.*, vol. 8, no. 1, Mar. 2021, Art. no. 2050048.
[27] I. Guo, G. Loeper, J. Obłój, and S. Wang, "Joint modeling and calibration of SPX and VIX by optimal transport," *SIAM J. Financial Math.*, vol. 13, no. 1, pp. 1–31, Mar. 2022.
[28] M. F. Dixon, I. Halperin, and P. Bilokon, *Machine Learning in Finance—From Theory To Practice*. Cham, Switzerland: Springer, 2020.
[29] B. Horvath, A. Muguruza, and M. Tomas, "Deep learning volatility: A deep neural network perspective on pricing and calibration in (rough) volatility models," *Quant. Finance*, vol. 21, no. 1, pp. 11–27, Jan. 2021.
[30] S. E. Rømer, "Empirical analysis of rough and classical stochastic volatility models to the SPX and VIX markets," *Quant. Finance*, vol. 22, no. 10, pp. 1805–1838, Oct. 2022.
[31] Y. Liu and Y. Wang, "Volatility estimation by combining stock price data and option data," *Statist. Interface*, vol. 6, no. 4, pp. 427–433, 2013.
[32] A. Gelman, J. B. Carlin, H. S. Stern, and D. B. Rubin, *Bayesian Data Analysis* (Texts in Statistical Science Series). London, U.K.: Chapman & Hall, 1995.
[33] W. R. Gilks, S. Richardson, and D. J. Spiegelhalter, *Markov Chain Monte Carlo in Practice* (Interdisciplinary Statistics). London, U.K.: Chapman & Hall, 1996.
[34] P. Diaconis, "The Markov chain Monte Carlo revolution," *Bull. Amer. Math. Soc.*, vol. 46, no. 2, pp. 179–205, 2009.
[35] M. D. Hoffman and A. Gelman, "The No-U-Turn sampler: Adaptively setting path lengths in Hamiltonian Monte Carlo," *J. Mach. Learn. Res.*, vol. 15, pp. 1593–1623, Apr. 2014.
[36] E. G. Phadia, "Nonparametric Bayesian estimation," in *Prior Processes and Their Applications* (Springer Series in Statistics), 2nd ed., Cham, Switzerland: Springer, 2016.
[37] D. Lewandowski, D. Kurowicka, and H. Joe, "Generating random correlation matrices based on vines and extended onion method," *J. Multivariate Anal.*, vol. 100, no. 9, pp. 1989–2001, Oct. 2009.
[38] M. R. Fengler and L.-Y. Hin, "Semi-nonparametric estimation of the call-option price surface under strike and time-to-expiry no-arbitrage constraints," *J. Econometrics*, vol. 184, no. 2, pp. 242–261, Feb. 2015.
[39] S. N. Cohen, C. Reisinger, and S. Wang, "Detecting and repairing arbitrage in traded option prices," *Appl. Math. Finance*, vol. 27, no. 5, pp. 345–373, Sep. 2020.
[40] R. H. Byrd, P. Lu, J. Nocedal, and C. Zhu, "A limited memory algorithm for bound constrained optimization," *SIAM J. Sci. Comput.*, vol. 16, no. 5, pp. 1190–1208, Sep. 1995.
[41] O. A. Martin, *Bayesian Analysis With Python: A Practical Guide to Probabilistic Modeling*, 3rd ed., Birmingham, U.K.: Packt Publishing, 2024.

NORRIS M. MULENGA received the B.S. degree in mathematics education from The Copperbelt University, Zambia, in 2014, and the Postgraduate Diploma degree in actuarial science from The University of Zambia, in 2018. He is currently pursuing the M.Phil. degree in statistics with Shandong University of Science and Technology, China.

During the M.Phil. studies, his research has focused on financial statistics, resulting in his thesis titled "Dynamic Calibration of the Black-Scholes Model by Bayesian Method Using Call and Put Options Data." This work involves developing advanced techniques for dynamically calibrating the Black-Scholes model, using Bayesian methods to enhance the model's accuracy and applicability with call and put options data.

YU FU received the B.S. degree in statistics and the Ph.D. degree in financial mathematics and financial engineering from Shandong University, Jinan, China, in 2010 and 2016, respectively.

Since 2016, he has been an Assistant Professor with the School of Mathematics and Systems Science, Shandong University of Science and Technology, Qingdao, China. His research interests include numerical methods for solving forward-backward stochastic differential equations and stochastic optimal control problems, uncertainty quantification, Bayesian inverse problems, and their applications in financial engineering.